High-Resolution, Spin-Echo BOLD, and CBF fMRI at 4 and 7 T

Timothy Q. Duong,* Essa Yacoub, Gregory Adriany, Xiaoping Hu, Kamil Ugurbil, J. Thomas Vaughan, Hellmut Merkle, and Seong-Gi Kim

With growing interest in noninvasive mapping of columnar organization and other small functional structures in the brain, achieving high spatial resolution and specificity in fMRI is of critical importance. We implemented a simple method for BOLD and perfusion fMRI with high spatial resolution and specificity. Increased spatial resolution was achieved by selectively exciting a slab of interest along the phase-encoding direction for EPI, resulting in a reduced FOV and number of phase-encoding steps. Improved spatial specificity was achieved by using SE EPI acquisition at high fields, where it is predominantly sensitive to signal changes in the microvasculature. Robust SE BOLD and perfusion fMRI were obtained with a nominal in-plane resolution up to 0.5 × 0.5 mm² at 7 and 4 Tesla, and were highly reproducible under repeated measures. This methodology enables high-resolution and high-specificity studies of functional topography in the millimeter to submillimeter spatial scales of the human brain. Magn Reson Med 48:589–593, 2002.

Key words: high resolution; spatial specificity; spin echo; brain mapping; FAIR; BOLD; high fields

Blood oxygenation level dependent (BOLD) (1) fMRI has been widely exploited to visualize brain function with a resolution of a few millimeters to a centimeter. While this spatial scale is suitable for a large number of cognitive and psychology questions, it is inadequate for studying functional parcellation at the millimeter or submillimeter level. Increasing spatial resolution generally requires a parallel increase in the data acquisition time. Because most fMRI studies utilize the echo-planar imaging (EPI) data acquisition scheme, it is not possible to sample the entire *k*-space with a large number of phase-encoding steps in a single excitation because of the T_2^* decay. Segmented *k*-space acquisition, partial-Fourier sampling (2), outer-volume suppression (3), and inner volume (voxel) selection (4–7) have been proposed.

In addition, simply obtaining images with high spatial resolution is inadequate if the signals that are being imaged do not have high *specificity* (i.e., accuracy of functional mapping). This is a problem in techniques like fMRI because electrical activity is imaged indirectly through metabolic and/or blood flow changes induced by that activity. The above-mentioned high-resolution imaging approaches have used gradient-echo (GE) BOLD contrast because of its high sensitivity. Because GE signals from draining venules and veins dominate, the intrinsic spatial resolution of GE BOLD fMRI is limited by vascular structures (8) and thus they may not be adequate for mapping submillimeter functional structures. Spin-echo (SE) imaging at high magnetic fields (9–12) and/or perfusion-based (13–16) acquisition can be used to increase spatial specificity. SE refocuses static intravoxel dephasing caused by a magnetic field gradient around large vessels, and thus eliminates their contribution to the BOLD response. Further, at high fields the intravascular BOLD contribution from large vessels is markedly reduced (11,12,17) due to the short T_2 of the venous blood. Therefore, SE BOLD fMRI at high (but not at low) fields is predominantly sensitive to BOLD changes originating largely from the *microvasculature.* Similarly, MR measurement of cerebral blood flow (CBF) can be targeted to parenchyma, avoiding large draining vein contributions because the majority of the magnetically labeled water in the capillaries exchanged with tissue water; while signal loss due to T_1 recovery reduces venous blood labeling by the time the blood reaches the draining veins. Improved spatial specificity with CBF fMRI (13–16) is sufficient to map individual cortical columns separated by about 1 mm (16).

In the present study, we implemented a simple method for achieving both high spatial specificity and high spatial resolution for fMRI applications at high magnetic fields. Increased spatial resolution was achieved by selectively refocusing a small slab, resulting in a reduced FOV and thus increased spatial resolution for a given matrix size. The slab selection was adapted from previous voxel-selective imaging schemes (4,5). Improved spatial specificity was based on using the Hahn SE (HSE) BOLD approach at high magnetic fields and CBF-based functional mapping. We demonstrated this methodology by performing single-shot, SE BOLD fMRI with a nominal in-plane resolution up to 0.5 × 0.5 mm², and single-shot, SE CBF fMRI up to 1 × 1 mm² resolution in the human brain at 4 and 7 Tesla.

METHODS

Seven healthy volunteers (22–35 years old) were studied with informed consent (four subjects at 7 T and three subjects at 4 T). For visual stimuli, flashing lights were presented via a 10-Hz LED matrix positioned 20–25 cm away from the eyes. For the motor task, the subjects were instructed to tap their fingers bilaterally at 2 Hz as cued via the LED goggles.

MR experiments were performed on a 7T/90 cm (Magnex Scientific, UK) or a 4T/90 cm (Oxford, UK) MRI scanner, driven by Varian's ^{unity}INOVA consoles (Palo Alto,

Center for Magnetic Resonance Research, Department of Radiology, University of Minnesota School of Medicine, Minneapolis, Minnesota.

Grant sponsor: NIH; Grant numbers: RR08079; NS38295; NS40719; MH55346; Grant sponsors: MIND Institute; Keck Foundation.

*Correspondence to: Timothy Q. Duong, Ph.D., Center for Comparative Neuroimaging, University of Massachusetts Medical Center, 55 Lake Ave. North, Worcester, MA 01655. E-mail: timothy.duong@umassmed.edu

Received 19 February 2002; revised 3 May 2002; accepted 16 May 2002.
DOI 10.1002/mrm.10252
Published online in Wiley InterScience (www.interscience.wiley.com).

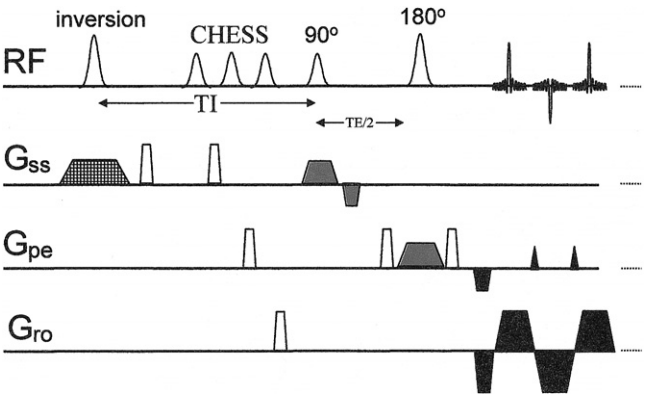

FIG. 1. Schematic representation of the SE, slab-selective EPI pulse sequence. The spatially-selective gradients (gray trapezoid) for the 90° and 180° pulses are placed on two orthogonal directions (slice-selection and phase-encoding direction), making it possible to select a slice and a slab, respectively. Three CHESS pulses followed by crusher gradients (2 G/cm for 2 ms, open trapezoid) are used for fat suppression. The inversion pulse shown with a slice-selective gradient (hatched trapezoid) is a 10-ms adiabatic, hyperbolic secant used in FAIR measurement. The phase-encoding and readout EPI gradients are shown in black triangles and trapezoids, respectively. RF, radiofrequency pulses; G_{ss}, gradient on slice-selection axis; G_{pe}, gradient on phase-encoding axis; G_{ro}, gradient on readout axis.

CA). The former was equipped with a Magnex head-gradient set (4 G/cm, 250 μs risetime) and the latter a Sonata body-gradient set (4 G/cm, 400 μs rise time; Siemens). A half-volume, quadrature surface coil (12-cm ID) was used at 7 T, and a TEM volume coil (27-cm ID) was used at 4 T (18).

All fMRI data were obtained using a single-shot, slab-selective EPI sequence shown in Fig. 1. Slab selection employed a single HSE acquisition scheme with two spatially selective gradients accompanying the excitation and refocusing pulses placed along two orthogonal directions: the slice-selective and phase-encoding axes. The slab thickness could thus be reduced, resulting in a reduced field of view (FOV) along the phase-encoding direction.

For BOLD imaging, SE, slab-selective EPI was acquired in a single shot using: TR = 2.0 s, TE = 60 ms at 4 T and 50 ms at 7 T, slice thickness = 1 or 2 mm, spectral width = 200–350 kHz, and matrix = 256 × 64. The acquisition time per *k*-space line was 1.0–1.5 ms (with ramp sampling). The slab thickness along the phase-encoding direction was 6 or 3 cm, and the FOV was 25.6 × 6.4 or 12.8 × 3.2 cm^2, corresponding to a nominal in-plane resolution of 1 × 1 or 0.5 × 0.5 mm^2, respectively. For the highest resolution (0.5 × 0.5 mm^2), partial Fourier acquisition with two extra *k*-space lines was used.

Perfusion-based fMRI was measured using flow-sensitive alternating inversion recovery (FAIR) (13), with slice-selective (ssIR) and non-slice-selective (nsIR) inversion-recovery images acquired in an interleaved fashion. The inversion pulse was followed by SE EPI acquisition after a delay TI. The thickness of the slice-selective inversion was three times the imaging slice thickness. The following parameters were employed: TR = 3.0 s, TE = 60 ms at 4 T and 40 ms at 7 T, TI = 1.2 s, slice thickness = 3 or 4 mm, and spectral width = 140–200 kHz. The acquisition time per *k*-space line was 1.0–1.5 ms (with ramp sampling). The slab thickness = 8 or 3 cm, FOV = 19.2 × 9.6 or 12.8 × 3.2 cm^2, and matrix = 128 × 64 or 128 × 32, corresponding to a nominal in-plane resolution of 1.5 × 1.5 mm^2 or 1 × 1 mm^2, respectively.

The TI value was experimentally optimized for CBF (subtraction) contrast in the brain parenchyma (data not shown). Although TR generally scales with the tissue T_1, we chose to keep TR at 7T to be the same as 4 T and optimized TI, which was also found to be 1.2 s.

Data Analysis

Images of cerebral blood flow (CBF) were obtained by pairwise, pixel-by-pixel subtraction of the nsIR images from the ssIR images. fMRI data analysis was performed using STIMULATE (19). Cross-correlation (CC) activation maps were computed with a typical CC threshold of 0.3. A minimal cluster size for an active region of 8 pixels was further imposed and the effective *P*-value was $< 10^{-4}$ for visualization. Activation maps were overlaid on the averaged HSE or inversion-recovery HSE EPI images. Pixel-by-pixel reproducibility was evaluated by comparing two sets of maps under repeated measures. Typically, two or four repeated fMRI measurements were made and equally divided into two groups, from which two activation maps were computed with the same statistical threshold and without using clustering of 8 pixels. Reproducibility was expressed as percent overlap of the average number of activated pixels of the individual maps.

RESULTS

Representative single-shot, HSE BOLD studies (7 T) of the visual cortex at 1 × 1 × 2 mm^3 and 0.5 × 0.5 × 2.0 mm^3 nominal resolution, and their corresponding time courses are shown in Fig. 2. Activated pixels are found predominantly in the gray matter, avoiding regions of white matter and cerebrospinal fluid. Reproducibility was evaluated and results for the HSE BOLD study at 1 × 1 × 2 mm^2 nominal resolution is shown in Fig. 2b. The reproducibility was 95% for the low-resolution and 60% for the high-resolution data sets. Similar reproducibility analysis was performed in the noise regions of the image outside the brain; the overlapped pixels due to chance constituted < 5%. The HSE BOLD percent changes range from 5–10% at 7 T. Increased percent change at the same statistical threshold was observed with higher spatial resolution.

Figure 3 shows two representative FAIR studies (7 T) obtained using single-shot, SE, slab-selective EPI at a nominal spatial resolution of 1.5 × 1.5 × 4.0 mm^3 (a–e) and 1 × 1 × 3 mm^3 (f–h). The FAIR images (Fig. 3a and f) show good perfusion contrast at basal conditions, with higher CBF contrast in the gray matter than in white matter and cerebrospinal fluid, as expected. Activation maps obtained using ssIR and CBF show increased activities predominantly localized to the gray matter, excluding regions of white matter and cerebrospinal fluid. A remarkable spatial correspondence was observed between the HSE ssIR (3b) and CBF map (3d). Reproducibility was evaluated for the ssIR map at 1.5 × 1.5 × 4.0 mm^2; ~80% of activated pixels overlapped.

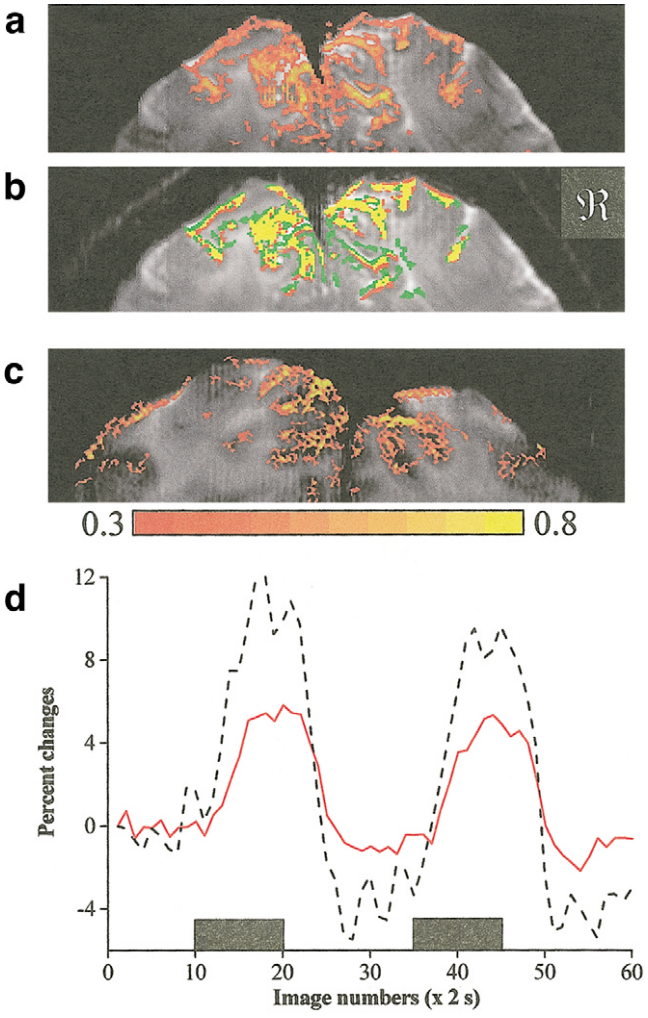

FIG. 2. Representative HSE BOLD fMRI using single-shot, slab-selective EPI at 7 T. **a:** HSE BOLD activation maps following visual stimulation at 1 × 1 × 2 mm^2 nominal spatial resolution. Slab thickness = 55 mm, matrix = 256 × 64, and FOV = 25.6 × 6.4. Note that the activation map is overlaid on an HSE BOLD EPI image. **b:** Reproducibility map of part **a**. Four repeated measurements were made and grouped into two sets: the first two and last two. Activation maps were calculated for each set (red and green pixels) and overlaid. The common pixels are shown in yellow. Approximately 95% of the activated pixels overlap. **c:** HSE BOLD activation maps following visual stimulation at 0.5 × 0.5 × 2.0 mm^2 nominal spatial resolution. The activation map is overlaid on an HSE IR-EPI image. Slab thickness = 30 mm, matrix = 256 × 64, and FOV = 12.8 × 3.2. Reproducibility was ~60% (data not shown). Color bar = cross-correlation coefficient ranging from 0.3 to 0.8. **d:** A representative time course from **a** is shown as a red solid trace, and from **c** as a dotted black trace.

The functional maps obtained by the difference between ssIR and nsIR images largely reflect CBF changes, although there could be some BOLD contamination. In our data, this contamination was minor because at the same statistical threshold the nsIR map (Fig. 3b) showed a much smaller (20 times) activation than the ssIR map (Fig. 3c). The former contains the same BOLD input but without the blood flow contribution. The percent change of the nsIR BOLD map (obtained with the ssIR activation map as a mask) was three to four times smaller than that of the ssIR map, again indicating that the BOLD contribution to the SE ssIR map was relatively small. Figure 3i shows the typical CBF percent changes ranging from 60–100%.

Similar high-resolution studies were also performed at 4 T with a volume coil following visual and motor tasks. Robust HSE BOLD maps at 1 × 1 × 2 mm^2 and 0.5 × 0.5 × 2 mm^2 nominal resolution were readily obtained (data not shown). Representative activation maps obtained using the ssIR scheme following visual and motor tasks are shown in Fig. 4. The reproducibility of the visual stimulation and the motor task were 70% and 71%, respectively.

DISCUSSION

The slab-selective approach is similar to the voxel-selection scheme (4–6), which uses three spatially selective pulses. Slab selection is less sensitive to refocusing (180°) pulse imperfection compared to voxel selection because only one (rather than two) refocusing pulse is used. With slab-selective EPI, high spatial resolution can be achieved in a single shot. Activation maps are highly reproducible and compare favorably with those obtained at 1.5 T (20) and 4 T (21) at low spatial resolution and using GE EPI. Without slab selection, achieving similar spatial resolution would have required four to 16 segments, resulting in an increased imaging time and potential segmentation artifacts. Slab-selective acquisition offers some advantages over the outer-volume-suppression technique: 1) it does not have the magnetization-transfer effect that is associated with a train of adiabatic pulses commonly used in signal suppression, and 2) it avoids potential problems with power deposition, particularly with volume-coil applications. One major disadvantage of the slab-selection approach for BOLD imaging is its relatively low temporal resolution. Another is that multislice acquisition in an interleaved fashion for whole-brain imaging is not practical.

High-resolution fMRI using single-shot acquisition results in long total readout time (approximately twice that of tissue T_2^*), resulting in blurring along the phase-encoding direction and effectively reducing spatial resolution. Preliminary analysis based on the Windischberger and Moser method (22) suggested that such blurring could be up to ~1 pixel. The long readout time also gives rise to T_2^* weighting in the SE EPI, especially in the high k-space lines. The spatial blurring and T_2^* effect due to the long readout time are currently under investigation. These problems can be alleviated by partial k-space and/or segmentation acquisition.

As in any high-resolution MRI, the signal-to-noise ratio (SNR) is a major issue. This methodology benefits significantly from the use of high magnetic fields because both the SNR and the contrast-to-noise ratio (CNR) increase at high fields. SNR improvement can be realized from improved RF coil design, such as the two-coil system (e.g., a large excitation coil and a small detection coil). Improved gradient performance in terms of magnitude and slew rate is also equally critical.

The spatial correspondence between the FAIR and ssIR maps is remarkable, and is indicative of negligible BOLD contributions from large draining veins in the CBF-

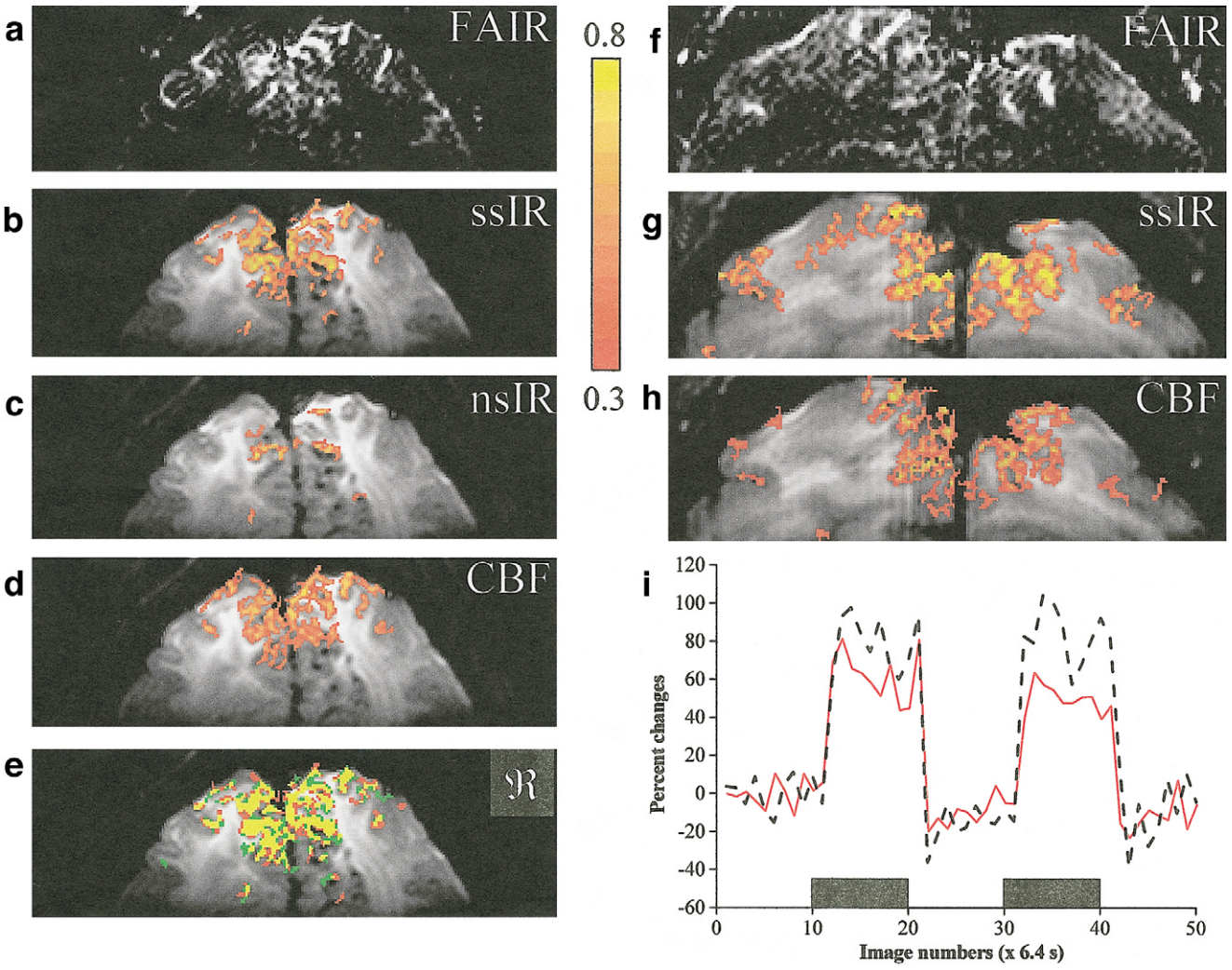

FIG. 3. Representative single-shot, SE FAIR studies of the visual cortex at 7 T. **a:** A FAIR image was obtained by subtracting the nsIR from the ssIR image. Activation maps were obtained from (**b**) slice-selective, inversion-recovery (ssIR) images, (**c**) non-slice-selective, inversion-recovery (nsIR) images, and (**d**) FAIR. Functional maps were overlaid on the nsIR image obtained as part of the FAIR measurements. The nominal spatial resolution was $1.5 \times 1.5 \times 4$ mm^3, FOV = 19.2×9.6 cm^2, and data matrix = 128×64. **e:** A reproducibility map of the ssIR map. Approximately 81% of the pixels (yellow) overlapped. **f–h:** A similar CBF fMRI study, except at higher ($1 \times 1 \times 3$ mm^3) spatial resolution, was obtained with FOV = 12.8×3.2 cm^2, and data matrix = 128×32. The color bar reflects the cross-correlation coefficient ranging from 0.3 to 0.8. **i:** Representative time courses of CBF changes for activation maps at $1.5 \times 1.5 \times 4$ mm^3 (solid red trace) and at $1 \times 1 \times 3$-mm^3 (dotted black trace) spatial resolution.

weighted ssIR maps because of SE acquisition. This observation suggests that paired-image acquisition for FAIR fMRI is not needed for CBF-weighted functional mapping with SE acquisition; the ssIR image alone is sufficient to yield CBF contrast if large-vessel BOLD components can be suppressed by using SE acquisition at high fields and/or minimizing the TE (i.e., using spiral data collection). The advantages of acquiring only the ssIR image at very short TEs include doubling of the temporal resolution, increases in SNR, and reduced physiological fluctuations in perfusion fMRI.

Marked increases in HSE BOLD and CBF percent changes were observed at high spatial resolution. This could be due to reduced partial volume effect and/or pixel "dropout" due to low SNR. Since both T_2 BOLD and CBF maps are expected to be highly specific and restricted to the gray matter, partial volume effect due to incomplete resolution of gray/white matter and cerebrospinal space is expected at the coarser resolution. Preliminary analyses indicated that the partial volume effect is substantial. Hyde et al. (8) have extensively investigated the issue of CNR for high-resolution T_2^* BOLD imaging at 3 T. They predicted that the optimal spatial resolution was a cubic voxel, and found experimentally an optimal spatial resolution of $1.5 \times 1.5 \times 1.5$ mm^2 for T_2^*-weighted fMRI at 3 T. They suggested that this resolution is determined by the anatomy of the vasculature, which shows small veins separated by ~1 mm in the cortex. Because of the improved specificity of CBF-based fMRI and the SE BOLD signals at higher fields, the intrinsic spatial resolution of these modalities is not dictated by the density of draining veins and large venules, but by spatial extents of the CBF response

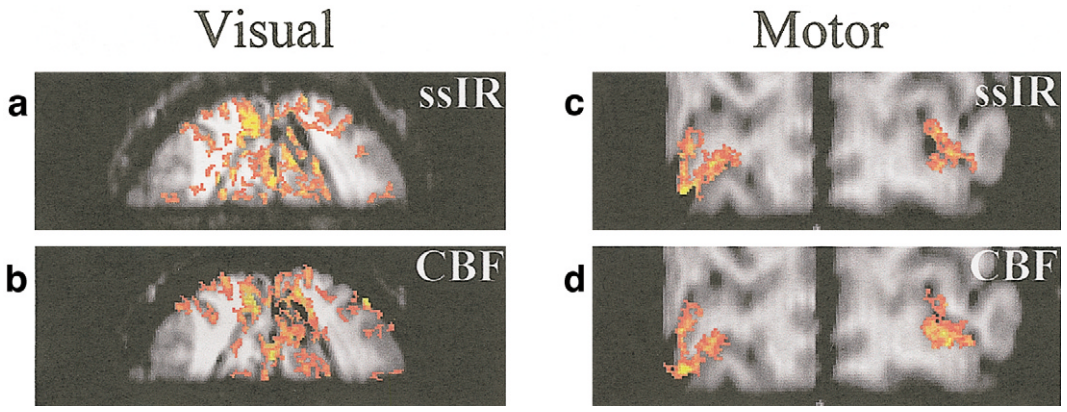

FIG. 4. Representative slab-selective fMRI at 4 T obtained using a volume coil. (**a**) Slice-selective IR (ssIR) and (**b**) CBF activation maps at $1.5 \times 1.5 \times 4.0$ mm^3 nominal resolution from the visual cortex. (**c-d**) Similar maps are shown for the motor task. Slab thickness = 80 mm, FOV = 19.2×9.6 cm^2, and data matrix = 128×64. The reproducibility of the visual stimulation and the motor task were 70% and 71%, respectively.

induced by neural activity. This notion, if confirmed, could have strong ramifications in pushing fMRI toward higher and higher functional resolutions.

CONCLUSIONS

SE BOLD and CBF fMRI in humans at a millimeter to submillimeter resolution was achieved by using slab selection in a single shot. Functional maps were highly reproducible under repeated measures. Increased spatial resolution yielded a marked increase in functional contrast relative to low resolution. This methodology has the potential to offer a unique platform for high-resolution and high-specificity fMRI of small functional structures.

REFERENCES

1. Ogawa S, Lee T-M, Kay AR, Tank DW. Brain magnetic resonance imaging with contrast dependent on blood oxygenation. Proc Natl Acad Sci USA 1990;87:9868–9872.
2. Haacke EM, Liang ZP, Boada F. Image reconstruction using projection onto convex sets, model constraints, and linear prediction theory for removal of phase, motion and Gibbs artifacts in magnetic resonance and ultrasound imaging. Optical Eng 1990;29:555–566.
3. Le Roux P, Gilles RJ, McKinnon GC, Carlier PG. Optimized outer volume suppression for single-shot fast spin-echo cardiac imaging. J Magn Reson Imaging 1998;8:1022–1032.
4. Feinberg DA, Hoenninger JC, Crooks LE, Kaufman L, Watts JC, Arakawa M. Inner volume MR imaging: technical concepts and their application. Radiology 1985;156:743–747.
5. Turner R, von Kienlin M, Moonen CT, van Zijl PC. Single-shot localized echo-planar imaging (STEAM-EPI) at 4.7 tesla. Magn Reson Med 1990;14:401–408.
6. Buecker A, Adam G, Neuerburg JM, Glowinski A, van Vaals JJ, Guenther RW. MR-guided biopsy using a T_2-weighted single-shot zoom imaging sequence (Local Look technique). J Magn Reson Imaging 1998; 8:955–959.
7. Yang Y, Mattay VS, Weinberger DR, Frank JA, Duyn JH. Localized echo-volume imaging methods for functional MRI. J Magn Reson Imaging 1997;7:371–375.
8. Hyde JS, Biswal BB, Jesmanowicz A. High-resolution fMRI using multislice partial *k*-space GR-EPI with cubic voxels. Magn Reson Med 2001;46:114–125.
9. Thulborn KR, Chang SY, Shen GX, Voyvodic JT. High-resolution echo-planar fMRI of human visual cortex at 3.0 Tesla. NMR Biomed 1997; 10:183–190.
10. Jovicich J, Norris DG. Functional MRI of the human brain with GRASE-based BOLD contrast. Magn Reson Med 1999;41:871–876.
11. Lee S-P, Silva AC, Ugurbil K, Kim S-G. Diffusion-weighted spin-echo fMRI at 9.4 T: microvascular/tissue contribution to BOLD signal change. Magn Reson Med 1999;42:919–928.
12. Duong TQ, Yacoub E, Adriany G, Hu X, Merkle H, Andersen P, Vaughan JT, Ugurbil K, Kim S-G. Diffusion-weighted BOLD fMRI at 4 and 7 Tesla: evaluation of micro- versus macrovascular contribution. In: Proceedings of the 9th Annual Meeting of ISMRM, Glasgow, Scotland, 2001. p 1253.
13. Kim S-G. Quantification of relative cerebral blood flow change by flow-sensitive alternating inversion recovery (FAIR) technique: application to functional mapping. Magn Reson Med 1995;34:293–301.
14. Kwong KK, Belliveau JW, Chesler DA, Goldberg IE, Weisskoff RM, Poncelet BP, Kennedy DN, Hoppel BE, Cohen MS, Turner R, Cheng H-M, Brady TJ, Rosen BR. Dynamic magnetic resonance imaging of human brain activity during primary sensory stimulation. Proc Natl Acad Sci USA 1992;89:5675–5679.
15. Detre JA, Leigh JS, Williams DS, Koretsky AP. Perfusion imaging. Magn Reson Med 1992;23:37–45.
16. Duong TQ, Kim D-S, Ugurbil K, Kim S-G. Localized blood flow response at sub-millimeter columnar resolution. Proc Natl Acad Sci USA 2001;98:10904–10909.
17. Yacoub E, Shmuel A, Pfeuffer J, van de Moortele P-F, Adriany G, Andersen P, Vaughan JT, Merkle H, Ugurbil K, Hu X. Imaging brain function in humans at 7 Tesla. Magn Reson Med 2001;45:588–594.
18. Vaughan JT, Hetherington HP, Otu JO, Pan JW, Pohost GM. High frequency volume coils for clinical NMR imaging and spectroscopy. Magn Reson Med 1994;32:206–218.
19. Strupp JP. Stimulate: a GUI based fMRI analysis software package. NeuroImage 1996;3:S607.
20. Noll DC, Genovese CR, Nystrom LE, Vazquez AL, Forman SD, Eddy WF, Cohen JD. Estimating test-retest reliability in functional MR imaging. II. Application to motor and cognitive activation studies. Magn Reson Med 1997;38:508–517.
21. Tegeler C, Strother SC, Anderson JR, Kim S-G. Reproducibility of BOLD-based functional MRI obtained at 4 T. Hum Brain Mapp 1999; 7:267–283.
22. Windischberger C, Moser E. Spatial resolution in echo planar imaging: shifting the acquisition window in *k*-space. Magn Reson Imaging 2000; 18:825.